Density Functional Investigation of High-Spin XY (X = Cr, Mo, W and Y = C, N, O) Molecules

F. Stevens,[†,‡] I. Carmichael,[*,§] F. Callens,[†] and M. Waroquier[‡]

Department of Solid State Sciences, Ghent University, Krijgslaan 281-S1 and Center for Molecular Modeling, Ghent University, Proeftuinstraat 86, B-9000 Ghent, Belgium, and Radiation Laboratory, University of Notre Dame, Notre Dame, Indiana 46556

Received: February 2, 2006

The performance of a density functional theory approach in calculating the equilibrium bond length, dipole moment, and harmonic vibrational frequency in a series of group 6 (Cr, Mo, W) transition metal-containing diatomic molecules is evaluated. Using flexible basis sets comprised of Slater type functions, a wide range of exchange-correlation functionals is investigated. Comparing with known experimental values and published results from high-level theoretical calculations, the most suitable functional form is selected. The importance of relativistic effects is checked, and predictions are made for several unknown dipole moments. The best agreement with experimental parameters is obtained when using a general gradient approximation, while special and hybrid functional forms give less accurate results.

1. Introduction

As a prelude to a computational study of the radiation chemistry of organic and water radicals interacting with transition metal (TM)-containing surfaces, we calibrate the performance of a Slater function-based density functional theory (DFT) approach on a set of simple diatomic TM and main group element-containing molecules.

Diatomic molecules containing elements in the first transition series have been heavily studied, both experimentally[1−8] and theoretically.[9−15] The methodological requirements, including both basis set flexibility and extent of electron correlation recovery, for reliable computational results have been the subject of a recent excellent review,[16] which also provided abundant interpretive examples of the TM−main group element bond. Reports on compounds involving TMs from the 4d row are much less common.[17−30] While several specific molecules have been observed and calculated, we know of no comparable systematic review of theoretical treatments. Recently, however, an exhaustive review of the performance of DFT for first and second row TM dimers has appeared.[31] Very little is known either experimentally[33−36] or theoretically[37−41] on diatomics containing TM elements from the 5d series where relativistic effects surely become important.

Here, we present results of calculations on some spectroscopic properties of the series of diatomic carbides, nitrides, and oxides of the group 6 TMs, Cr, Mo, and W. A wide range of exchange-correlation functionals is explored, including local, gradient-corrected, and hybrid versions. Basis set considerations are discussed, and relativistic effects are also taken into account.

2. Computational Details

To find the most appropriate functional form that satisfactorily describes the whole set of molecules, 22 exchange-correlation forms, which can be grouped in five different classes, are considered. The five classes of functionals are as follows: (i) the local density approximation (LDA), (ii) general gradient approximation (GGA), (iii) meta-GGA, (iv) special functionals that have the correct asymptotic behavior, and (v) hybrid functionals. The present DFT calculations are performed using the Amsterdam density functional (ADF) program package,[42−44] version 2004, and the Gaussian2003 (G03) program package.[45] Exchange correlation forms, which belong to the first four classes, are studied using the ADF program package. In particular, the following functionals are applied in the present study: (i) LDA, VWN[46] and Stoll VWN;[46,47] (ii) GGA, Bp86,[48,49] Pw91,[50,51] BLYP,[49,52−54] OLYP,[52−55] mPW,[50,60] PBE,[51] and OPBE;[51,55] (iii) meta-GGA, all meta-forms of the previous GGA functionals;[57−63] and (iv) special forms, Lb94[64] and SAOP.[65] All of these functionals are combined with the following full electron zero order regular approximation basis sets: single-ζ (SZ), double-ζ (DZ), double-ζ with polarization function (DZP), triple-ζ with polarization function (TZP), triple-ζ with two polarization functions (TZ2P), and a quadrupole-ζ with four polarization functions (QZ4P).

The G03 program package is employed when using functional forms out of the fifth class. Hybrid functionals are considered as follows: B3LYP,[66] B3PW91,[50,51,66] B3P86,[48,66] and BHandHLYP.[67] These functional forms are used in combination with the following basis sets: 3-21G,[68] 6-31G,[69] 6-31G*,[69] WTBS,[70,71] and LanL2DZ.[72−76]

Multiconfigurational self-consistent field calculations within the complete active space (CASSCF) method employing the Dalton suite of electronic structure programs[77] are used to estimate the configurational composition of the predicted electronic ground states (GSs).

Finally, before calculating a spectroscopic property using a particular basis set and functional form combination, the geometry of the molecule under consideration is optimized at that particular level of theory. For some functional forms (meta-GGA and special functionals), analytic geometry optimizations are not currently possible. In these cases, a pointwise scan was

* To whom correspondence should be addressed. E-mail: carmichael.1@nd.edu.
[†] Department of Solid State Sciences, Ghent University.
[‡] Center for Molecular Modeling, Ghent University.
[§] University of Notre Dame.

10.1021/jp060717u CCC: $33.50 © 2006 American Chemical Society
Published on Web 03/18/2006

TABLE 1: Overview of Earlier Theoretical Calculations Performed on the XY Molecules[a]

molecule	ref	method	μ (D)	r_e (Å)	ω_e (cm^{-1})
CrC	2	DFT/LSDA	n.a.	1.557	1050
CrC	2	DFT/BPW91	n.a.	1.593	n.a.
CrC	2	DFT/B3LYP	5.58	1.642	637
CrC	2	RCCSD	n.a.	1.602	n.a.
CrC	2	UCCSD	n.a.	1.636	n.a.
CrC	2	CASSCF	7.12	1.659	662
CrC	2	MRCI	6.84	1.676	675
CrC	2	ROHF	n.a.	1.488	n.a.
CrC	1	CASSCF	n.a.	n.a.	542
MoC	21	MRCI	n.a.	1.688	997
WC	33	MRCI	4.21	1.727	977.5
WC	35	CASSCF	n.a.	1.744	968.5
WC	35	FOCI	n.a.	1.747	937.0
CrN	9	MRCI	2.08	1.619	n.a.
CrN	10	MRCI	2.00	1.619	854
CrN	11	CCSD(T)	2.96	1.541	1018
CrN	11	CCSD(T) + MVD	3.20	1.537	1076
MoN	24	CASSCF	1.991	1.643	1070
MoN	24	MRCI	2.11	1.636	1109
MoN	22	GVB RCI	3.123	1.603	1100
WN	35	CASSCF	n.a.	1.696	1026.1
WN	35	FOCI	n.a.	1.700	1022.2
CrO	12	CASSCF	n.a.	1.86	630
CrO	12	MRCI	n.a.	1.660	820
CrO	4	CASSCF	3.19	1.649	855
CrO	4	MRCI	3.752	1.63	853
CrO	4	MRCI + Q	3.8	1.634	853
CrO	15	DFT/BPW91	n.a.	1.61	903
CrO	13	DFT/JMW	3.66	1.6	996
CrO	13	DFT/VWN	3.76	1.6	976
CrO	13	DFT/BVWN	4.01	1.64	884
CrO	13	DFT/BPW	3.82	1.63	961
CrO	14	DFT/BPW91	3.64	1.611	911
CrO	14	DFT/BLYP	3.74	1.622	903
CrO	14	DFT/B3LYP	4.24	1.615	870
MoO	12	SDCI	n.a.	1.71	1035
MoO	29	TDDFT/B3LYP	n.a.	1.75	902
MoO	26	DFT/PWVWN	n.a.	1.72	882
WO	41	CMRCI	1.72	1.672	1050

[a] For each molecule, the obtained internuclear distance r_e (in Å), dipole moment μ (in Debye), vibrational frequency ω_e (in cm^{-1}), the applied computational method, and the corresponding reference are given.

performed when varying the internuclear distance in order to obtain the configuration that is lowest in energy. Also, when using special functionals (Lb94 and SAOP), the computation of the vibrational frequency is not possible in ADF and is therefore not reported.

3. Computational Results

3.1. Benchmarking DFT Methods: CrN and CrO Molecules. In this section, we benchmark our DFT results against experimental and published high-level computational data. In Table 1, an overview of all previous computational results of the molecules under consideration is given. The choice of CrN and CrO as test cases to calibrate our DFT calculations is motivated by the fact that both molecules have been extensively investigated in recent years, both experimentally and theoretically.

Electronic Structure. Prior to any spectroscopic calculation, we check if the applied theoretical method is able to reproduce the experimental GS. Relative energies, referred to as the electronic configuration that is lowest in energy, of various electronic configurations for carbides (singlet, triplet, and quintet), nitrides (doublet, quartet, and sextet), and oxides (singlet, triplet, quintet, and septet) are listed in Table 2. The

TABLE 2: Determination of the GS Configuration of the XY (X = Cr, Mo, W and Y = C, N, O) Molecules[a]

		Cr		Mo		W	
	2S + 1	ΔE (eV)	GS	ΔE (eV)	GS	ΔE (eV)	GS
C	1	1.569	$^1\Gamma$	1.065	$^1\Gamma$	3.237	$^1\Sigma^+$
C	3	0.0	$^3\Sigma^-$	0.0	$^3\Sigma^-$	0.0	$^3\Delta$
C	5	0.369	$^5\Sigma^-$	1.139	$^5\Sigma^-$	0.958	$^5\Sigma^-$
N	2	0.769	$^2\Delta$	0.792	$^2\Delta$	0.656	$^2\Delta$
N	4	0.0	$^4\Sigma^-$	0.0	$^4\Sigma^-$	0.0	$^4\Sigma^-$
N	6	2.777	$^6\Sigma^-$	3.798	$^6\Sigma^-$	3.931	$^6\Sigma^-$
O	1	3.632	$^1\Sigma^+$	1.496	$^1\Sigma^+$	0.917	$^1\Sigma^+$
O	3	0.911	$^3\Sigma^-$	0.568	$^3\Sigma^-$	0.0	$^3\Sigma^-$
O	5	0.0	$^5\Pi$	0.0	$^5\Pi$	0.742	$^5\Pi$
O	7	2.129	$^7\Pi$	2.809	$^7\Pi$	4.277	$^7\Pi$

[a] For each molecule, the corresponding GS is given and all energies are referred to the configuration that is lowest in energy. All values are in eV. All calculations were performed using the Bp86 functional form in combination with a QZ4P basis set. For the WY molecules, SR corrections were considered.

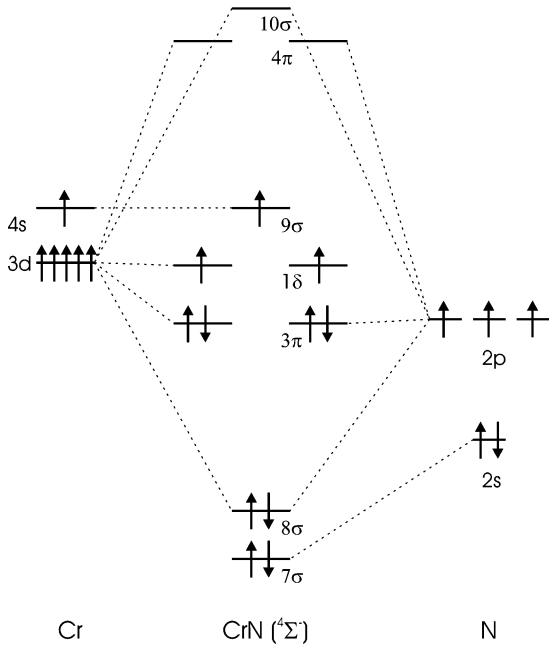

Figure 1. Molecular orbital diagram for CrN.

TABLE 3: GS Electronic Configuration of the XY (X = Cr, Mo, W and Y = C, N, O) Molecules, Using DFT Methods

molecule	electronic configuration	GS
CrC	$(7\sigma)^2(3\pi)^4(8\sigma)^2(1\delta)^2$	$^3\Sigma^-$
CrN	$(7\sigma)^2(8\sigma)^2(3\pi)^4(1\delta)^2(9\sigma)^1$	$^4\Sigma^-$
CrO	$(7\sigma)^2(8\sigma)^2(3\pi)^4(1\delta)^2(9\sigma)^1(4\pi)^1$	$^5\Pi$
MoC	$(10\sigma)^2(5\pi)^4(11\sigma)^2(2\delta)^2$	$^3\Sigma^-$
MoN	$(10\sigma)^2(11\sigma)^2(5\pi)^4(2\delta)^2(12\sigma)^1$	$^4\Sigma^-$
MoO	$(10\sigma)^2(11\sigma)^2(5\pi)^4(2\delta)^2(12\sigma)^1(6\pi)^1$	$^5\Pi$
WC	$(14\sigma)^2(8\pi)^4(15\sigma)^2(16\sigma)^1(4\delta)^1$	$^3\Delta$
WN	$(14\sigma)^2(8\pi)^4(15\sigma)^2(16\sigma)^1(4\delta)^2$	$^4\Sigma^-$
WO	$(14\sigma)^2(15\sigma)^2(8\pi)^4(16\sigma)^2(4\delta)^2$	$^3\Sigma^-$

present DFT calculations (using the Bp86 functional form in combination with a QZ4P basis set) predict the GS to be $^4\Sigma^-$ for CrN and $^5\Pi$ for CrO, in agreement with experimental results.[4,12] The obtained ordering and occupation of the molecular orbitals for the CrN molecule in the $^4\Sigma^-$ GS are illustrated in Figure 1. A similar ordering and occupation was obtained by Balfour et al.,[5] by comparing experimental and MRCI data. These results give confidence to the corresponding predictions of the other molecules listed in Table 2. Table 3 lists the orbital composition of the dominant electronic configuration in these predicted ground electronic states.

TABLE 4: Weight of the Dominant Configuration in the GS Wave Function (Defined as "c") from CASSCF/3-21G Calculations[a]

molecule	GS	c	molecule	GS	c	molecule	GS	c
CrC	$^3\Sigma^-$	0.859	CrO	$^5\Pi$	0.891	MoN	$^4\Sigma^-$	0.906
CrN	$^4\Sigma^-$	0.866	MoC	$^3\Sigma^-$	0.899	MoO	$^5\Pi$	0.929

[a] For each molecule, the corresponding GS is given.

TABLE 5: Influence of Basis Set Effects, Using the Bp86 Functional Form, on Computed Spectroscopic Data of the CrN and CrO Molecules Using Both the ADF and the G03 Program Package

	CrN			CrO		
basis set	μ (D)	r_e (Å)	ω_e (cm^{-1})	μ (D)	r_e (Å)	ω_e (cm^{-1})
exp.	2.31[a]	1.571	1050	3.88[b]	1.615	898
SZ	3.414	1.458	1448.4	4.428	1.487	847.4
DZ	3.517	1.582	957.0	4.259	1.650	869.2
DZP	3.298	1.562	996.0	3.893	1.624	916.8
TZP	3.173	1.558	988.7	3.777	1.621	920.7
TZ2P	3.081	1.545	1022.1	3.695	1.612	925.1
QZ4P	2.939	1.543	1016	3.531	1.611	920.3
3-21G	3.293	1.507	1168.0	2.567	1.584	1067.9
6-31G	3.264	1.538	1062.7	3.380	1.618	962.4
6-31G*	3.245	1.535	1070.5	3.226	1.590	999.8
WTBS	2.918	1.546	1064.3	3.373	1.618	983.1
LanL2DZ	2.837	1.529	1041.9	3.565	1.604	924.1

[a] Ref 7. [b] Ref 4.

CASSCF Calculations on the GS Electronic Configuration. DFT is inherently a single configuration approach to electron structure. It is thus of interest to investigate the extent to which each of the predicted electronic GSs can in fact be represented by a single configurational wave function. To this end, we report the results from CASSCF calculations on these states in Table 4 for the CrX and MoX molecules. These calculations were performed with the 3-21G basis set correlating the 2s and 2p electrons on the main group element and the outer ns and n-1d shells on the TM atom. The 3-21G basis set is of split-valence quality comprising [3s2p] on C, N, and O, [5s4p2d] on Cr, and [6s5p3d] on Mo contractions of larger primitive Gaussian sets. The bond lengths for states of each multiplicity were optimized analytically, and at the optimized geometry, the coefficient of the leading configuration for the particular state is listed in Table 4. For all considered molecules, the CAS results predict the same electronic GSs.

Influence of Basis Set. It is also important to investigate the influence of basis set effects on the DFT calculations. The advantage of using the ADF program package is that very large all-electron basis sets, up to the QZ4P level, can be applied for all TMs under consideration. Adopting the Bp86 functional, we see from Table 5 that when increasing the basis set size from SZ to QZ4P, convergence in the computed spectroscopic properties for both the CrN and the CrO molecules is found. While the dipole moment seems to be most affected by basis set effects, only small variations in the internuclear distance and the vibrational frequency are observed when increasing the flexibility of the basis. For both CrN and CrO, the dipole moment decreases when increasing the basis set, leading to a larger deviation from experiment for the CrO molecule. Because all computed spectroscopic values are reasonably converged as a function of basis set size when using a QZ4P basis set and the agreement with experimental data is reasonably close, this basis set was employed in all further calculations using the ADF program package.

A limited number of Gaussian basis sets is available for heavy elements in the G03 program package (especially for 4d and 5d TMs). From the results listed in Table 5, it can be noticed that the calculated properties are moderately influenced by basis set effects with the exception of the dipole moment. The pseudopotential-based LanL2DZ basis provides results in reasonable accord with the extensive Slater function (TZ2P or QZ4P basis sets) predictions and will therefore be used in the following. This is also the choice for Gaussian basis set calculations most frequently employed in the literature.[29]

TABLE 6: Computed Spectroscopic Properties of the CrN Molecule Using 22 Different Exchange Correlation Forms

functional class	XC form	μ (D)	r_e (Å)	ω_e (cm^{-1})
	exp.[a]	2.31	1.571	1050
LDA	VWN	2.841	1.520	1097.5
LDA	SVWN	2.798	1.528	1085.5
GGA	Bp86	2.939	1.543	1016.0
GGA	BLYP	3.041	1.553	1010.4
GGA	Pw91	2.962	1.541	1025.3
GGA	mPW	2.974	1.546	1009.8
GGA	PBE	3.054	1.542	1029.7
GGA	OLYP	3.053	1.558	893.3
GGA	OPBE	2.904	1.527	989.8
meta-GGA	Bp86	2.942	1.545	1010.4
meta-GGA	BLYP	3.040	1.553	1010.1
meta-GGA	Pw91	2.967	1.542	1023.2
meta-GGA	mPW	2.970	1.545	1013.1
meta-GGA	PBE	3.098	1.546	1014.1
meta-GGA	OLYP	2.999	1.547	932.6
meta-GGA	OPBE	3.009	1.541	937.5
special	SAOP	3.791	1.525	n.a.
special	Lb94	3.604	1.532	n.a.
hybrid	B3LYP	3.067	1.539	838.4
hybrid	B3P86	2.990	1.526	881.8
hybrid	B3PW91	2.971	1.538	813.8
hybrid	BHandHLYP	3.513	1.736	498.9

[a] Ref 7.

Variation of Exchange Correlation Form. We have also tested the performance of a wide variety of exchange-correlation functional forms. These can be characterized as belonging to five different classes (see section 2 above). Because of the large amount of computational data, we only report the results for all 22 of these functional forms for the CrN molecule (Table 6), although a similar investigation was performed for all other molecules. As is clear from the results listed in Table 6, the variation of the computed data within a particular class of functionals is rather small. The only exception is the BHandHLYP functional in the class of hybrid functionals. The latter form gives results, which strongly deviate from the computed data of all other hybrid functionals. Therefore, we select a particular functional form out of each class that gives the closest overall agreement with experimental data and is representative for the entire class: LDA, SVWN; GGA, Bp86; meta-GGA, meta-Bp86; special, Lb94; and hybrid, B3LYP. Although this choice is based on the computational results of the CrN molecule, a similar conclusion can be made when comparing the theoretical results from all 22 functional forms on all other molecules. For all other XY molecules, computational results using these selected representatives of each class of functionals are presented in Table 7.

First, we shall focus on the CrN molecule. As is clear from the results listed in Table 7, all spectroscopic properties are strongly affected by the functional form used. Although the SVWN functional gives the closest agreement with the experimental dipole moment, the best overall agreement with all experimental spectroscopic data is obtained when using the Bp86 functional form. While the meta-Bp86 form gives comparable

TABLE 7: Overview of the Computational Results Using Five Different Classes of Functionals[a]

	XC	CrC	CrN[b]	CrO[c]	MoC[d]	MoN[e]	MoO[f]	WC[g]	WN	WO[j]
μ	SVWN	5.341	2.798	3.333	5.218	2.546	2.629	4.016	3.791	1.882
μ	Bp86	5.431	2.939	3.531	5.209	2.606	2.893	4.065	3.906	1.912
μ	meta-Bp86	5.434	2.942	3.533	5.200	2.593	2.726	4.040	3.848	1.862
μ	B3LYP	5.749	3.067	4.208	3.145	2.835	3.435	4.206	4.263	2.538
μ	Lb94	4.718	3.604	3.429	5.080	3.439	4.016	3.744	4.111	3.571
μ	exp.	**n.a.**	**2.31**	**3.88**	**n.a.**	**2.44**	**n.a.**	**n.a.**	**3.77**[h]	**n.a.**
r_e	SVWN	1.641	1.528	1.593	1.657	1.623	1.695	1.694	1.652	1.648
r_e	Bp86	1.589	1.543	1.611	1.667	1.634	1.710	1.725	1.669	1.658
r_e	meta-Bp86	1.599	1.545	1.612	1.645	1.614	1.708	1.701	1.670	1.660
r_e	B3LYP	1.717	1.539	1.614	1.713	1.608	1.701	1.736	1.691	1.676
r_e	Lb94	1.556	1.532	1.586	1.661	1.625	1.709	1.697	1.665	1.620
r_e	exp.	**n.a.**	**1.571**	**1.615**	**1.676**	**1.648**	**1.70**	**1.714**	**1.668**[h]	**1.658**
ω_e	SVWN	775.7	1085.5	969.8	1063.1	1104.4	949.3	1055.1	1127.5	1100.7
ω_e	Bp86	925.8	1016.0	920.3	1034.7	1068.6	916.1	989.7	1083.5	1155.4
ω_e	meta-Bp86	916.2	1010.4	919.4	1084.5	1119.2	906.6	954.6	1080.1	1078.3
ω_e	B3LYP	578.3	838.4	846.7	1058.3	1134.7	949.9	988.1	1082.8	1066.5
ω_e	exp.	**n.a.**	**1050**	**898**	**1008.3**	**1075**	**893.5**	**983.2**	**1060**[i]	**1064.6**

[a] For all molecules, the internuclear distance r_e (in Å), dipole moment μ (in Debye), and vibrational frequency ω_e (in cm^{-1}) are given. The corresponding reference of the experimental values is given in the top of the table. [b] Ref 7. [c] Ref 4. [d] Ref 18. [e] Ref 23. [f] Ref 25. [g] Ref 34. [h] Ref 36. [i] Ref 32. [j] Ref 41.

accuracy to Bp86, the use of hybrid or special functional forms widens the separation from experiment. Comparing our Bp86 DFT results to high-level MRCI and coupled cluster (CC) data is very instructive because these theoretical data can then be used to calibrate the accuracy of the present DFT results. As is clear from the data listed in Table 1, MRCI calculations[10] underestimate the experimental dipole moment (2.00 as compared to 2.31 D), overestimate the internuclear distance (1.619 as compared to 1.571 Å), and underestimate the vibrational frequency (854 as compared to 1050 cm^{-1}). CCSD calculations[11] overestimate the experimental dipole moment, while the internuclear distance is underestimated and the computed vibrational frequency is perhaps fortuitously in close accord with the experimentally observed value. Generally, we can conclude that the present Bp86 DFT results give similar accuracy when compared to these high-level MRCI and CCSD calculations, at least when applied to the CrN molecule.

To further calibrate our DFT approach, the CrO molecule is also investigated in detail. As for CrN, the computational results are strongly dependent on the applied functional form. While excellent agreement with experimental data is obtained when using the Bp86 functional (and the meta-Bp86 form), the use of hybrid and special forms is not recommended. Comparing our DFT results with the DFT data of Veliah et al.[13] and Gutsev et al.[14] on CrO (Table 1), similar conclusions can be made: excellent agreement with experimental data when using a GGA functional and failure of the hybrid B3LYP functional. When benchmarking our DFT results against high-level MRCI+Q data of Steimle et al.,[4] the same conclusions as for the CrN molecule can be made as follows: MRCI results give a better agreement with the experimental dipole moment, while DFT gives slightly better accord with the measured vibrational frequency and internuclear distance.

Dissociation Energy. In Figure 2, the binding energy and dipole moment of the CrN molecule are plotted as a function of the internuclear distance using the Bp86 functional form in combination with a QZ4P basis set. Note that to obtain the bond energy of CrN, correction terms as suggested by Baerends et al.[78] were applied. As is clear from this figure, the dipole moment is a very sensitive function of the internuclear distance. A similar dependence of the dipole moment was reported by Shim et al.[24] for the MoN molecule in CASSCF calculations. On the basis of Figure 2, the estimated dissociation energy for

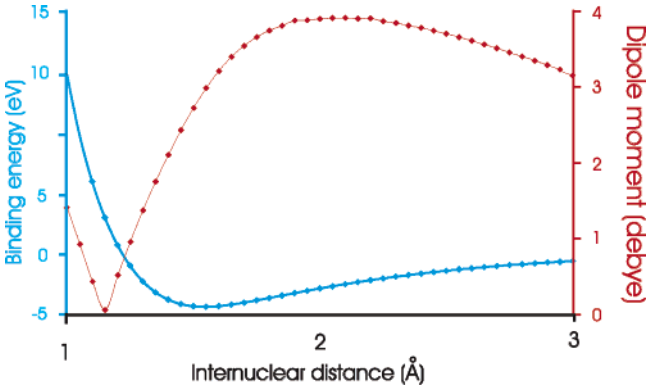

Figure 2. Variation of the dipole moment and the binding energy of the CrN molecule as a function of the internuclear distance.

TABLE 8: Computed Spectroscopic Data of the CrN Molecule for Both the Nonrelativistic (NR) and the SR Cases

		SVWN		Bp86		meta-Bp86	
	exp.[a]	NR	SR	NR	SR	NR	SR
μ (D)	2.31	2.939	2.989	2.962	3.019	2.942	3.015
r_e (Å)	1.571	1.543	1.526	1.541	1.538	1.545	1.542
ω_e (cm^{-1})	1050	1016	1051.5	1025.3	993.1	1010.4	1027.9

[a] Ref 7.

CrN is 4.6 eV, which is larger than the experimental value of 3.9 eV.[79] The previous procedure was also applied on the CrO molecule. A similar dependence of the dipole moment as a function of the internuclear distance was observed. The estimated dissociation energy of 5.2 eV is again larger than the experimental value of 4.78 eV.[80]

Scalar Relativistic (SR) Effects. The influence of SR effects on the computed spectroscopic data of the CrN molecule is investigated in Table 8. The presented results indicate that SR effects have only a minor influence on the computed spectroscopic data. Because of these relativistic effects, the dipole moment increases by about 0.05 D, only slightly depending on the applied functional form. A similar increase in dipole moment when adding SR effects was observed by Jansik et al.,[11] when performing CCSD(T) calculations on CrN. For all employed levels of theory, SR effects tend to shorten the bond length, which was also observed by Liu et al.[81] While relativistic effects have only a small influence on the internuclear distance and

TABLE 9: Influence of SR Effects on the Computed GS Spectroscopic Properties of WY (Y = C, N, O) Molecules

			SVWN		Bp86		meta-Bp86	
molecule		exp.	NR	SR	NR	SR	NR	SR
WC	μ (D)	n.a.	5.185	4.016	5.170	4.065	5.166	4.040
WC	r_e (Å)	1.714[a]	1.693	1.694	1.706	1.724	1.703	1.701
WC	ω_e (cm^{-1})	983.2	1052.9	1055.1	1016.9	989.7	1024	954.6
WN	μ (D)	3.77[b]	2.842	3.791	3.229	3.905	3.007	3.848
WN	r_e (Å)	1.660	1.660	1.652	1.677	1.669	1.672	1.670
WN	ω_e (cm^{-1})	n.a.	1086.7	1127.5	1077.7	1083.5	1054.4	1080.1
WO	μ (D)	n.a.	2.357	1.882	1.633	1.912	2.449	1.862
WO	r_e (Å)	1.658[c]	1.669	1.648	1.686	1.658	1.661	1.660
WO	ω_e (cm^{-1})	1064.6	1150.2	1100.7	996.0	1155.4	1064.8	1078.4

[a] Ref 34. [b] Ref 36. [c] Ref 41.

dipole moment, larger variations are observed in the computed vibrational frequencies, although the change is strongly dependent on the functional form employed. While for the SVWN and meta-Bp86 functionals the computed vibrational frequency increases when relativistic effects are included, relativistic effects tend to decrease this frequency in the case of the Bp86 functional. Generally, we can conclude that SR effects have only a small influence on the computed spectroscopic data of CrN. A similar investigation was performed on the CrO molecule, and the same conclusions could be made.

3.2. Further Validation: XN and XO Molecules. The previous discussion suggests that DFT can be usefully applied in the description of high-spin TM systems. Nevertheless, further testing and calibration are needed. For this reason, a similar procedure as performed above is applied to the MoN, MoO, WN, and WO molecules. While we mainly focused on the "level of theory" (basis set, functional form, relativistic effects, etc.) in the previous section, we now discuss in detail the performance of DFT in comparison with experimental data and previous high-level computational results.

MoN and MoO Molecules. We first check if DFT is able to predict the correct GS for MoN and MoO. While a $^4\Sigma^-$ GS is obtained for MoN, a $^5\Pi$ GS is retrieved for the MoO molecule (Table 2). Both computational results are confirmed by experiment.[22−25] The GS electronic configuration of both molecules is presented in Table 3. As for the Cr-containing molecules, the computed spectroscopic data are highly dependent on the applied functional form (Table 7). While the SVWN and (meta-)Bp86 functionals give comparable accuracy, the use of hybrid or special functional forms gives inaccurate results. The best overall agreement with experimental data is obtained when using the Bp86 functional form. Therefore, this functional form shall be used in the following discussion. We also investigated the influence of SR effects on the computed spectroscopic values. As in the case for CrN and CrO, these effects have only a very small influence and are therefore not considered for these molecules.

As is clear from the data listed in Table 7, our DFT Bp86 results for MoN are in good agreement with the available experimental data. While the experimental dipole moment is slightly overestimated and the internuclear distance is somewhat underestimated, the computed vibrational frequency is in perfect agreement with the experimental value. Computed spectroscopic data for MoN, which resulted from an MRCI calculation by Shim et al.,[24] gave reasonable accord with experiment, although the computed dipole moment of 2.11 D is significantly smaller than the experimental value of 2.44 D. When comparing the accuracy of DFT and MRCI methods, DFT prediction is then superior. To our knowledge, no experimental value for the dipole moment of MoO has been reported. Also, no theoretical prediction for this property is available.[12,26,29] Because of the close agreement with experimental results for the MoN molecule, we believe that the computed dipole moment of 2.8 D is a reliable estimate of the real value for MoO. As for MoN, the computed DFT values for the internuclear distance and the vibrational frequency are in close agreement with the experimental results. When comparing our DFT results and the SDCI data of Bauschlicher et al.[12] with experimental data for MoO, the same accuracy is obtained, although our computed vibrational frequency is closer to the experimental value.

WN and WO Molecules. It is frequently reported that predicting properties of third row TM molecules, especially those containing tungsten, is challenging because of the added relativistic effects.[19,36] The computed GS configurations for WN and WO are listed in Tables 2 and 3. While for the WN molecule the $^4\Sigma^-$ GS is found, the $^3\Sigma^-$ GS is predicted for WO. These DFT predictions are supported by experiment.[36,41] The influence of SR effects on the computed spectroscopic data is presented in Table 9. Irrespective of the functional form employed, the introduction of these effects has a very large influence on the computed dipole moment, shifting it toward the experimental value for the WN molecule. In all cases, adding relativistic effects tend to shorten the bond length. While the vibrational frequency is only slightly affected in case of the WN molecule, a larger fluctuation is observed in case of the WO molecule. Because of the significant impact of relativistic effects on the computed spectroscopic data of WN and WO, these effects are systematically included in all further calculations concerning these molecules. From the five classes of functionals that are considered here (Table 7), the calculated properties using the GGA Bp86 form give the closest agreement with the available experimental data.

Predictions for WN are in close accord with experimental values. While the dipole moment is slightly overestimated, the internuclear distance is perfectly reproduced. To our knowledge, there are no other theoretical predictions for the dipole moment of WN. CASSCF and FOCI methods[35] tend to overestimate the experimental bond length (Table 1). When comparing the general accuracy of our DFT Bp86 results for the WN molecule with those from FOCI calculations, we state that DFT is somewhat superior to the FOCI results.

For the WO molecule, the dipole moment has apparently not been determined experimentally. The present DFT value of 1.91 D is close to that of Ram et al.[41] of 1.72 D, which was obtained by a high-level CMRCI calculation. For the other spectroscopic properties, the DFT results are in closer accord with the experimentally determined values as referred to in the CMRCI results.

3.3. X-Carbides. Contrary to the case for the XN and XO (X = Cr, Mo, W) molecules, experimental spectroscopic

properties of the XC molecules are relatively scarce. There is no experimental study available concerning the CrC molecule, while the dipole moments for the MoC and WC molecules are also missing. From a theoretical point of view, the CrC molecule has been studied using a whole range of methods (Table 1), while computational studies concerning the MoC and WC molecules are very limited.

CrC Molecule. The GS for the CrC molecule is predicted to be $^3\Sigma^-$ (Table 2). A similar conclusion was made by Shim and Gingerich[1] from CASSCF calculations and confirmed by Maclagan et al.[2] using DFT, CASSCF, and MRCI computational techniques. Because the Bp86 functional form gave the closest agreement with experimental data for all considered XY molecules up to this point, the computed spectroscopic data using this functional form are discussed in the following. For completeness, computational results using functional forms out of all five classes are listed in Table 7. As for CrN and CrO, relativistic effects have only a very small influence on the computed spectroscopic data. Our computed dipole moment values of 5.43 (Bp86) and 5.74 D (B3LYP) are in close agreement with the B3LYP value of 5.58 D, reported by Maclagan et al.[2] When comparing these DFT data to CASSCF and MRCI values (Table 1), it can be observed that the latter techniques give very large dipole moments ($\approx$7 D). When further comparing our DFT results with the MRCI data reported in ref 2, it is observed that DFT gives a much smaller internuclear distance and a larger vibrational frequency. Further experimental work is required to resolve these discrepancies and decide which approximation gives the most satisfactory description of the CrC molecule.

MoC Molecule. The predicted GS configuration of MoC is $^3\Sigma^-$ (Table 2), in agreement with the conclusions made in ref 18. As for all other Cr and Mo molecules, relativistic effects have only a minor influence on the computed spectroscopic properties of the MoC molecule and are therefore not considered. Comparing the computed results of all five functional classes (Table 7) with the available experimental properties (internuclear distance and vibrational frequency), the best performance is achieved by the GGA Bp86 form: Both properties are perfectly reproduced by this method. Experimentally, no value of the dipole moment has been reported to our knowledge. Using an MRCI technique, the MoC molecule was investigated theoretically by Shim et al.,[21] although no dipole value was provided. Therefore, our prediction of 5.2 D is the first estimate of this spectroscopic property. When comparing the performance of the present DFT approach with the other MRCI data reported by Shim et al.,[21] we can conclude that both techniques give a similar accuracy.

WC Molecule. The calculated $^3\Delta$ GS for the WC molecule (Table 2) is in agreement with the experimental work of Sickafoose et al.[34] Because SR effects were seen to be important for both WN and WO, their influence is also investigated here and the results are displayed in Table 9. The introduction of relativistic effects significantly reduces the computed dipole moment, tends to increase the bond length, and, depending on the functional form employed, increases or decreases the vibrational frequency. As compared to the experimental data, the Bp86 functional form again produces the closest agreement with the available experimental data (Table 7).

Because of the lack of any experimental prediction of the dipole moment for the WC molecule, we have to compare our DFT value of 4.06 D with the MRCI result of 4.21 D reported by Balasubramanian.[33] Because both methods give approximately the same result, it is reasonable to assume that the experimental value will be in this vicinity. Also, the obtained internuclear distance reported in ref 33 (Table 1) is almost the same as those obtained by DFT methods. The vibrational frequency, which is always well-reproduced in other molecules considered here, is also in this case in excellent agreement with experiment. MRCI[33] or FOCI[35] techniques also produce excellent agreement with the experimental data, similar in accuracy to the present DFT results.

4. Discussion

While in the previous sections all molecules were investigated separately, we shall now focus on the performance of DFT over the whole range of XY molecules when varying the X (X = Cr, Mo, W) or the Y (Y = C, N, O) component. Also, the accuracy of DFT methods, as compared to experimental and high-level computational methods, is discussed. Prior to this discussion, a comment concerning the influence of relativistic effects on the computed spectroscopic properties is made.

Because of SR effects, the dipole moment of WC decreases while for WN and WO it increases (Table 9). This holds for Bp86. However, for WO, the change is opposite with meta-Bp86. Similar irregularities hold for the vibrational frequency. As a consequence, it is not straightforward to make final conclusions about relativistic effects and particularly on trends for different molecules less transparent.

Because of the limited number of experimental dipole moments, it is difficult to make final statements concerning the performance of DFT on this spectroscopic value. Generally, the Bp86 functional form gave close agreement with the available experimental data. In those cases where comparisons with high-level MRCI data could be made, reasonable agreement was achieved. We therefore state that the predicted dipole moments of the MoC and MoO molecules, which are unknown both from experimental or from theoretical points of view, are good estimates of the real values.

Contrary to the dipole moment, the internuclear distance is known experimentally for all XY molecules (except for the CrC molecule). Considering the experimental values, the following trends are observed when varying the ligand (C, N, O) of a particular TM atom: The internuclear distance decreases when going from MoC $\rightarrow$ MoN and WC $\rightarrow$ WN $\rightarrow$ WO and increases in the cases CrN $\rightarrow$ CrO and MoN $\rightarrow$ MoO. The following dependencies are noticed when varying the TM: an increase in internuclear distance when going from CrN $\rightarrow$ MoN $\rightarrow$ WN, MoC $\rightarrow$ WC, and CrO $\rightarrow$ MoO and a decrease in the case of MoO $\rightarrow$ WO. All of the latter observations are reproduced by the present DFT Bp86 calculations, which strongly support the present approach. As compared to MRCI techniques, which tend to overestimate the latter property, the computed DFT internuclear distances are in closer agreement with experiment.

Although large changes in the dipole moments and equilibrium internuclear distances are noticed when comparing the XY molecules, the vibrational frequencies of these molecules show only a small variation. When varying the ligand of a particular TM, the largest experimental vibrational frequency is observed for the X-nitrides. This is reproduced computationally for the Cr and Mo molecules. When increasing the size of the TM atom (Cr $\rightarrow$ Mo $\rightarrow$ W) for a particular ligand, the experimental frequencies tend to increase, except when going from CrO $\rightarrow$ MoO and MoC $\rightarrow$ WC. As for all other spectroscopic properties, DFT methods perfectly reproduce the previous trends. High-level MRCI methods also give an excellent description of the vibrational frequency, and the accuracy obtained is similar to that provided by the present DFT calculations.

5. Conclusion

The present DFT calculations on the spectroscopic properties (internuclear distance, vibrational frequency, and dipole moment) of nine different high-spin XY TM molecules by using five classes of functional forms allow us to estimate the reliability of these methods and draw definite conclusions on the values of some unknown spectroscopic data. For all considered molecules, the GGA Bp86 functional form gave the closest overall agreement with the available experimental data. Also, when comparison with high-level MRCI calculations was possible, it was found that the accuracy of both methods (DFT and MRCI) was similar.

Generally, we can conclude that DFT is a reliable method for studying high-spin TM molecules. Therefore, because of the low computational cost and relatively high accuracy, it can be used as a first method to investigate unknown systems before high-level MRCI calculations are performed. These results also lend confidence to adopting this approach to our further investigation of radical−surface interactions.

Acknowledgment. We thank the Fund for Scientific Research (FWO-Flanders, Belgium) for financial support. The research described herein was supported by the Office of Basic Energy Sciences of the U.S. Department of Energy. This is contribution NDRL-4618 from the Notre Dame Radiation Laboratory.

References and Notes

(1) Shim, I.; Gingerich, K. A. *Int. J. Quantum Chem.* **1992**, *42*, 349.
(2) Maclagan, R. G. A. R.; Scuseria, G. E. *J. Chem. Phys.* **1997**, *106*, 1491.
(3) Gutsev, G. L.; Andrews, L.; Bauschlicher, C. W. *Theor. Chem. Acc.* **2003**, *109*, 298.
(4) Steimle, T. C.; Nachman, D. F.; Shirley, J. E.; Bauschlicher, C. W.; Langhoff, S. R. *J. Chem. Phys.* **1989**, *91*, 2049.
(5) Balfour, W. J.; Qian, C. X. W.; Zhou, C. *J. Chem. Phys.* **1997**, *106*, 4383.
(6) Zhou, C.; Balfour, W. J.; Qian, C. X. W. *J. Chem. Phys.* **1997**, *107*, 4473.
(7) Steimle, T. C.; Robinson, J. S.; Goodridge, D. *J. Chem. Phys.* **1999**, *110*, 881.
(8) Namiki, K. C.; Steimle, T. C. *J. Chem. Phys.* **1999**, *111*, 6385.
(9) Blomberg, M. R. A.; Siegbahn, P. E. M. *Theor. Chim. Acta* **1992**, *81*, 365.
(10) Harrison, J. F. *J. Phys. Chem.* **1996**, *100*, 3513.
(11) Jansik, B.; Kello, V.; Urban, M. *Int. J. Quantum Chem.* **2002**, *90*, 1240.
(12) Bauschlicher, C. W.; Nelin, C. C.; Bagus, P. S. *J. Chem. Phys.* **1985**, *82*, 3265.
(13) Veliah, S.; Xiang, K.; Pandey, R.; Recio, J. M.; Newsam, J. M. *J. Phys. Chem. B* **1998**, *102*, 1126.
(14) Gutsev, G. L.; Rao, B. K.; Jena, P. *J. Phys. Chem. A* **2000**, *104*, 5374.
(15) Gutsev, G. L.; Jena, P.; Zhai, H.; Wang, L. *J. Chem. Phys.* **2001**, *115*, 7935.
(16) Harrison, J. F. *Chem. Rev.* **2000**, *100*, 679.
(17) Gupta, S. K.; Gingerich, K. A. *J. Chem. Phys.* **1981**, *74*, 3584.
(18) Brugh, D. J.; Ronningen, T. J.; Morse, M. D. *J. Chem. Phys.* **1998**, *109*, 7851.
(19) Li, X.; Liu, S. S.; Chen, W.; Wang, L. S. *J. Chem. Phys.* **1999**, *111*, 2464.
(20) DaBell, R. S.; Meyer, R. G.; Morse, M. D. *J. Chem. Phys.* **2001**, *114*, 2938.
(21) Shim, I.; Gingerich, K. A. *J. Chem. Phys.* **1997**, *106*, 8093.
(22) Allison, J. N.; Goddard, W. A. *Chem. Phys.* **1983**, *81*, 263.
(23) Fletcher, D. A.; Steimle, T. C. *J. Chem. Phys.* **1993**, *99*, 901.
(24) Shim, I.; Gingerich, K. A. *J. Mol. Struct.: TheoChem* **1999**, *460*, 123.
(25) Gunion, R. F.; Dixon-Warren, S. J.; Lineberger, W. C.; Morse, M. D. *J. Chem. Phys.* **1996**, *104*, 1765.
(26) Broclawik, E.; Salahub, D. R. *Int. J. Quantum Chem.* **1994**, *52*, 1017.
(27) Loock, H. P.; Simard, B.; Wallin, S.; Linton, C. *J. Chem. Phys.* **1998**, *109*, 8980.
(28) Tsipis, A. C. *Phys. Chem. Chem. Phys.* **2000**, *2*, 1357.
(29) Broclawik, E.; Borowski, T. *Chem. Phys. Lett.* **2001**, *339*, 433.
(30) Oliveira, J. A.; De Almeida, W. B.; Duarte, H. A. *Chem. Phys. Lett.* **2003**, *372*, 650.
(31) Schultz, N. E.; Zhao, Y.; Truhlar, D. G. *J. Phys. Chem. A* **2005**, *109*, 4388.
(32) Andrews, L.; Souter, P. F.; Bare, W. D.; Liang, B. *J. Phys. Chem. A* **1999**, *103*, 4649.
(33) Balasubramanian, K. *J. Chem. Phys.* **2000**, *112*, 7425.
(34) Sickafoose, S. M.; Smith, A. W.; Morse, M. D. *J. Chem. Phys.* **2002**, *116*, 993.
(35) Gao, X. M.; Liu, S. X.; Xie, X. G.; Cao, H.; Dai, S. S. *Chin. Chim. Lett.* **2001**, *12*, 655.
(36) Steimle, T. C.; Virgo, W. L. *J. Chem. Phys.* **2004**, *121*, 12411.
(37) Nelin, C. J.; Bauschlicher, C. W. *Chem. Phys. Lett.* **1985**, *118*, 221.
(38) Lorenz, M.; Agreiter, J.; Caspary, N.; Bondybey, V. E. *Chem. Phys. Lett.* **1998**, *291*, 291.
(39) Kraus, D.; Saykally, R. J.; Bondybey, V. E. *Chem. Phys. Lett.* **1998**, *295*, 285.
(40) Lorenz, M.; Bondybey, V. E. *Chem. Phys.* **1999**, *241*, 127.
(41) Ram, R. S.; Lievin, J.; Li, G.; Hirao, T.; Bernath, P. F. *Chem. Phys. Lett.* **2001**, *343*, 437.
(42) Guerra, C. F.; Snijders, J. G.; te Velde, G. T.; Baerends, E. J. *Theor. Chem. Acc.* **1998**, *99*, 391.
(43) te Velde, G. T.; Bickelhaupt, F. M.; van Gisbergen, S. J. A.; Fonseca, C.; Baerends, E. J.; Snijders, J. G.; Ziegler, T. *J. Comput. Chem.* **2001**, *22*, 931.
(44) ADF2004.01, SCM, Theoretical Chemistry, Vrije Universiteit, Amsterdam, The Netherlands, http://www.scm.com.
(45) Frisch, M. J.; Trucks, G. W.; Schlegel, H. B.; Scuseria, G. E.; Robb, M. A.; Cheeseman, J. R.; Montgomery, J. A., Jr.; Vreven, T.; Kudin, K. N.; Burant, J. C.; Millam, J. M.; Iyengar, S. S.; Tomasi, J.; Barone, V.; Mennucci, B.; Cossi, M.; Scalmani, G.; Rega, N.; Petersson, G. A.; Nakatsuji, H.; Hada, M.; Ehara, M.; Toyota, K.; Fukuda, R.; Hasegawa, J.; Ishida, M.; Nakajima, T.; Honda, Y.; Kitao, O.; Nakai, H.; Klene, M.; Li, X.; Knox, J. E.; Hratchian, H. P.; Cross, J. B.; Bakken, V.; Adamo, C.; Jaramillo, J.; Gomperts, R.; Stratmann, R. E.; Yazyev, O.; Austin, A. J.; Cammi, R.; Pomelli, C.; Ochterski, J. W.; Ayala, P. Y.; Morokuma, K.; Voth, G. A.; Salvador, P.; Dannenberg, J. J.; Zakrzewski, V. G.; Dapprich, S.; Daniels, A. D.; Strain, M. C.; Farkas, O.; Malick, D. K.; Rabuck, A. D.; Raghavachari, K.; Foresman, J. B.; Ortiz, J. V.; Cui, Q.; Baboul, A. G.; Clifford, S.; Cioslowski, J.; Stefanov, B. B.; Liu, G.; Liashenko, A.; Piskorz, P.; Komaromi, I.; Martin, R. L.; Fox, D. J.; Keith, T.; Al-Laham, M. A.; Peng, C. Y.; Nanayakkara, A.; Challacombe, M.; Gill, P. M. W.; Johnson, B.; Chen, W.; Wong, M. W.; Gonzalez, C.; Pople, J. A. *Gaussian 03*, revision B.3; Gaussian, Inc.: Wallingford, CT, 2004.
(46) Vosko, S. H.; Wilk, L.; Nusair, M. *Can. J. Phys.* **1980**, *58*, 1200.
(47) Stoll, H.; Pavlidou, C. M. E.; Preuss, H. *Theor. Chim. Acta* **1978**, *49*, 143.
(48) Perdew, J. P. *Phys. Rev. B* **1986**, *33*, 8822.
(49) Becke, A. D. *Phys. Rev. A* **1988**, *38*, 3098.
(50) Perdew, J. P.; Chevary, J. A.; Vosko, S. H.; Jackson, K. A.; Pederson, M. R.; Singh, D. J.; Fiolhais, C. *Phys. Rev. B* **1992**, *46*, 6671.
(51) Perdew, J. P.; Burke, K.; Ernzerhof, M. *Phys. Rev. Lett.* **1996**, *77*, 3865.
(52) Lee, C.; Yang, W.; Parr, R. G. *Phys. Rev. B* **1988**, *37*, 785.
(53) Johnson, B. G.; Gill, P. M. W.; Pople, J. A. *J. Chem. Phys.* **1993**, *98*, 5612.
(54) Russo, T. V.; Martin, R. L.; Hay, P. J. *J. Chem. Phys.* **1994**, *101*, 7729.
(55) Handy, N. C.; Cohen, A. *J. Mol. Phys.* **2001**, *99*, 403.
(56) Adamo, C.; Barone, V. *J. Chem. Phys.* **1998**, *108*, 664.
(57) Proynov, E. I.; Sirois, S.; Salahub, D. R. *Int. J. Quantum Chem.* **1997**, *64*, 427.
(58) Filatov, M.; Thiel, W. *Mol. Phys.* **1997**, *91*, 847.
(59) van Voorhis, T.; Scuseria, G. E. *J. Chem. Phys.* **1998**, *109*, 400.
(60) Filatov, M.; Thiel, W. *Phys. Rev. A* **1998**, *57*, 189.
(61) Krieger, J. B. In *Electron Correlations and Materials Properties*; Gonis, A., Kioussis, N., Eds.; Plenum: New York, 1999.
(62) Perdew, J. P.; Kurth, S.; Zupan, A.; Blaha, P. *Phys. Rev. Lett.* **1999**, *82*, 5179.
(63) Proynov, E. I.; Chermette, H.; Salahub, D. R. *J. Chem. Phys.* **2000**, *113*, 10113.
(64) van Leeuwen, R.; Baerends, E. J. *Phys. Rev. A* **1994**, *49*, 2421.
(65) Schipper, P. R. T.; Gritsenko, O. V.; van Gisbergen, S. J. A.; Baerends, E. J. *J. Chem. Phys.* **2000**, 112, 1344.
(66) Becke, A. D. *J. Chem. Phys.* **1993**, *98*, 5648.
(67) Frisch, A.; Frisch, M. J.; Trucks, G. W. *Gaussian 03 Users Reference*; Gaussian Inc.: Pittsburgh, PA, 2003.
(68) Dobbs, K. D.; Hehre, W. J. *J. Comput. Chem.* **1987**, *8*, 861.
(69) Rassolov, V.; Pople, J. A.; Ratner, M.; Windus, T. L. *J. Chem. Phys.* **1998**, *109*, 1223.

(70) Huzinaga, S.; Miguel, B. *Chem. Phys. Lett.* **1990**, *175*, 289.
(71) Huzinaga, S.; Klobukowski, M. *Chem. Phys. Lett.* **1993**, *212*, 260.
(72) Dunning, T. H., Jr.; Hay, P. J. In *Methods of Electronic Structure, Theory*; Schaefer, H. F., III, Ed.; Plenum Press: New York, 1977; Vol. 2.
(73) Hay, P. J.; Wadt, W. R. *J. Chem. Phys.* **1985**, *82*, 270.
(74) Hay, P. J.; Wadt, W. R. *J. Chem. Phys.* **1985**, *82*, 284.
(75) Hay, P. J.; Wadt, W. R. *J. Chem. Phys.* **1985**, *82*, 299.
(76) Ortiz, J. V.; Hay, P. J.; Martin, R. L. *J. Am. Chem. Soc.* **1992**, *114*, 2736.
(77) *DALTON, A Molecular Electronic Structure Program*, Release 2.0; 2005; http://www.kjemi.uio.no/software/dalton/dalton.html.
(78) Baerends, E. J.; Branchadell, V.; Sodupe, M. *Chem. Phys. Lett.* **1997**, *265*, 481.
(79) Gingirich, R. A. *J. Chem. Phys.* **1968**, *49*, 19.
(80) Merer, A. J. *Annu. Rev. Phys. Chem.* **1989**, *40*, 407.
(81) Liu, W.; Franke, R. *J. Comput. Chem.* **2001**, *23*, 564.